Corrections

ECOLOGY. For the article "Continental diatom biodiversity in stream benthos declines as more nutrients become limiting," by Sophia I. Passy, which appeared in issue 28, July 15, 2008, of *Proc Natl Acad Sci USA* (105:9663–9667; first published July 3, 2008; 10.1073/pnas.0802542105), the author notes two printer's errors. In the Abstract, line 4, the phrase "I tested whether niche dimensionality and, with this species, richness scale positively with NLR in running waters" should instead read: "I tested whether niche dimensionality and, with this, species richness, scale positively with NLR in running waters." In addition, in Table 1, the column 6 and 7 headings **NH_4-N** and **NO_3-N** should instead appear as **NH_4-N** and **NO_3-N**, respectively. The corrected table appears below.

Table 1. Nutrient concentrations in milligrams per liter (iron in μg/liter) measured in the NAWQA study streams across the three habitats

Habitat	Statistic	BC	SiO_2	Fe	NH_4-N	NO_3-N	P_{diss}
All	*Threshold*	*51.022*	*5.007*	*20**	*0.0213*	*0.245*	*0.011*
RTH, N = 1,189	Minimum	2.5	0.10	3	0.002	0.000	0.001
	Maximum	2,080	64	4,400	17.000	21.940	4.600
	Median	72.90	8.82	15.06	0.027	0.460	0.030
	Mean	94.38	11.02	86.62	0.082	1.360	0.115
DTH, N = 759	Minimum	2.50	0.10	3	0.002	0.000	0.003
	Maximum	1,069.30	64	2,600	17.000	13.714	4.600
	Median	68.27	9.10	17.69	0.030	0.471	0.030
	Mean	86.04	11.36	80.17	0.088	1.338	0.124
Phytoplankton, N = 330	Minimum	4.76	0.06	3	0.010	0.020	0.004
	Maximum	2,080.32	53	940	6.300	10.300	1.200
	Median	97.20	6.80	19.00	0.035	0.930	0.045
	Mean	120.86	8.66	71.37	0.096	1.534	0.100

BC, basic cations; P_{diss}, dissolved phosphorus. Concentrations below the given thresholds were determined to be limiting to eutrophic diatoms based on regression tree models (Table S1) or *literature data (47). *N*, number of observations.

www.pnas.org/cgi/doi/10.1073/pnas.0807088105

PHYSIOLOGY. For the article "TASK channel deletion in mice causes primary hyperaldosteronism," by Lucinda A. Davies, Changlong Hu, Nick A. Guagliardo, Neil Sen, Xiangdong Chen, Edmund M. Talley, Robert M. Carey, Douglas A. Bayliss, and Paula Q. Barrett, which appeared in issue 6, February 12, 2008, of *Proc Natl Acad Sci USA* (105:2203–2208; first published February 4, 2008; 10.1073/pnas.0712000105), the authors note that on page 2204, right column, line 18, the statement "a recent study reports sex differences in effects of TASK-1 subunit deletion on adrenal development and zonation; males appear normal, and females show marked developmental abnormalities (**25**)" is misreferenced and should instead cite ref. **48**. The added reference appears below.

48. Heitzmann D, *et al.* (2008) Invalidation of TASK1 potassium channels disrupts adrenal gland zonation and mineralocorticoid homeostasis. *Embo J* 27:179–187.

www.pnas.org/cgi/doi/10.1073/pnas.0807268105

BIOPHYSICS. For the article "Shifting transition states in the unfolding of a large ankyrin repeat protein," by Nicolas D. Werbeck, Pamela J. E. Rowling, Vasuki R. Chellamuthu, and Laura S. Itzhaki, which appeared in issue 29, July 22, 2008, of *Proc Natl Acad Sci USA* (105:9982–9987; first published July 16, 2008; 10.1073/pnas.0705300105), the authors note that, due to a printer's error, on page 9985, left column, 3 lines from the bottom, "The data are consistent with a model in which **TS2** has repeats 2–6 folded (as well as repeats 7–12 folded) and **TS** has only repeats 5 and 6 folded (as well as repeats 7–12 folded)" should instead read: "The data are consistent with a model in which **TS1** has repeats 2–6 folded (as well as repeats 7–12 folded) and **TS2** has only repeats 5 and 6 folded (as well as repeats 7–12 folded)."

www.pnas.org/cgi/doi/10.1073/pnas.0807474105

Shifting transition states in the unfolding of a large ankyrin repeat protein

Nicolas D. Werbeck*, Pamela J. E. Rowling, Vasuki R. Chellamuthu, and Laura S. Itzhaki†

MRC Cancer Cell Unit, Hutchison/MRC Research Centre, Hills Road, Cambridge CB2 0XZ, United Kingdom

Edited by Jose N Onuchic, University of California at San Diego, La Jolla, CA, and approved May 6, 2008 (received for review June 6, 2007)

The 33-amino-acid ankyrin motif comprises a β-turn followed by two anti-parallel α-helices and a loop and tandem arrays of the motif pack in a linear fashion to produce elongated structures characterized by short-range interactions. In this article we use site-directed mutagenesis to investigate the kinetic unfolding mechanism of D34, a 426-residue, 12-ankyrin repeat fragment of the protein ankyrinR. The data are consistent with a model in which the N-terminal half of the protein unfolds first by unraveling progressively from the start of the polypeptide chain to form an intermediate; in the next step, the C-terminal half of the protein unfolds via two pathways whose transition states have either the early or the late C-terminal ankyrin repeats folded. We conclude that the two halves of the protein unfold by different mechanisms because the N-terminal moiety folds and unfolds in the context of a folded C-terminal moiety, which therefore acts as a ''seed'' and confers a unique directionality on the process, whereas the C-terminal moiety folds and unfolds in the context of an unfolded N-terminal moiety and therefore behaves like a single-domain ankyrin repeat protein, having a high degree of symmetry and consequently more than one unfolding pathway accessible to it.

parallel pathways | protein engineering | protein folding | D34

Repeat proteins are a distinct class of structures that comprise tandem arrays of 30- to 50-residue structural motifs, frequently having high sequence identity between them, which pack in a relatively linear manner to form elongated structures stabilized by local interactions between residues close in sequence (1–4). They differ in this respect from globular protein structures, which have complex topologies and are stabilized by sequence-distant interactions. Because of the simplicity of this modular architecture, repeat proteins have been used successfully as scaffolds for engineering binding specificities (5, 6); proteins containing consensus repeats have been produced with enhanced stabilities compared with their natural counterparts (7–13), and we have found that their folding pathways are also amenable to design (14).

We have chosen a much larger repeat protein than has been previously investigated. D34 is a 12-ankyrin repeat fragment from the 24-ankyrin repeat domain of ankyrinR (Fig. 1). AnkyrinR is a multidomain protein that links a diverse set of proteins to the membrane-associated spectrin-actin cytoskeleton. The ankyrin domain has been shown to mediate many of these protein–protein interactions including those with ion channels, calcium release channels, and cell adhesion molecules (15). The folding and unfolding of large ankyrin repeat arrays is of particular interest because these proteins are thought to play a role in mechanical signal transduction by virtue of their putative elastic properties (16–18).

We previously analyzed the equilibrium unfolding of D34 by circular dichroism (CD) and by fluorescence of the single tryptophan residue located in the middle of the protein in the loop between the sixth and seventh repeats (19) (Fig. 1). We found that D34 populated a hyperfluorescent intermediate on urea-induced unfolding. In the intermediate the C-terminal half of the molecule was folded and the N-terminal half unfolded. Whereas the unfolding of the N-terminal repeats appeared to be cooperative, the unfolding of the C-terminal repeats was not. The protein responded to mutations in the N-terminal repeats in the same way as does a globular protein. The response to mutations in the C-terminal repeats, however, was unanticipated. The unfolding mechanism changed; the mutations caused the intermediate populated by the wild-type protein to be destabilized and different intermediates became predominant. The closer to the C terminus the mutation, the fewer C-terminal repeats were folded in the intermediate. We proposed a very rough energy landscape for the unfolding of D34, with many partly folded species of similar energy that contain different numbers of folded C-terminal repeats; thus, the intermediate species that dominates can easily be changed by relatively minor perturbations such as point mutations.

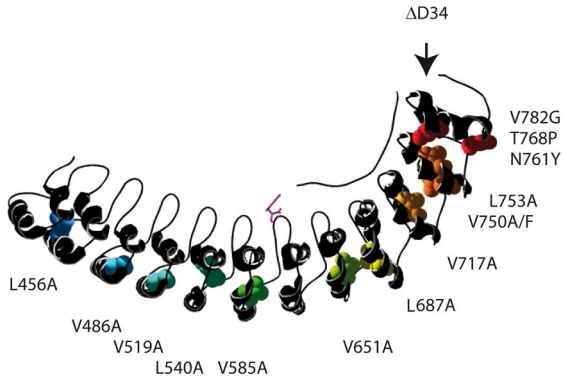

Fig. 1. Schematic representation of the structure of D34 (37), showing the single tryptophan and the mutated residues (figure created by using Swiss PDB Viewer and POV-Ray).

Here, the kinetics of unfolding and refolding of D34 is investigated by using 16 mutant variants. We find that the protein unfolds via an intermediate that has many properties in common with the equilibrium intermediate of the wild-type protein. The urea dependence of the transitions between native, intermediate, and unfolded states, and the effects of mutations on these profiles, are consistent with a model in which the N-terminal half of D34 unfolds with a broad energy barrier whereby repeats peel away from the end of the polypeptide chain toward the middle; subsequently, the C-terminal half unfolds via one of two parallel pathways, involving unraveling from one end of the structure or the other. The accessibility of alternative kinetic pathways may be a property of repeat proteins that distinguishes them from globular proteins, arising from the symmetry in their structures. Such behavior was

Author contributions: N.D.W. and P.J.E.R. contributed equally to this work; N.D.W. and L.S.I. designed research; N.D.W., P.J.E.R., V.R.C., and L.S.I. performed research; N.D.W., P.J.E.R., and L.S.I. analyzed data; and N.D.W. and L.S.I. wrote the paper.

The authors declare no conflict of interest.

This article is a PNAS Direct Submission.

See Commentary on page 9853.

*Present address: Max Planck Institute for Medical Research, Department of Biomolecular Mechanisms, Jahnstrasse 29, 69120 Heidelberg, Germany.

†To whom correspondence should be addressed. E-mail: lsi10@cam.ac.uk.

This article contains supporting information online at www.pnas.org/cgi/content/full/0705300105/DCSupplemental.

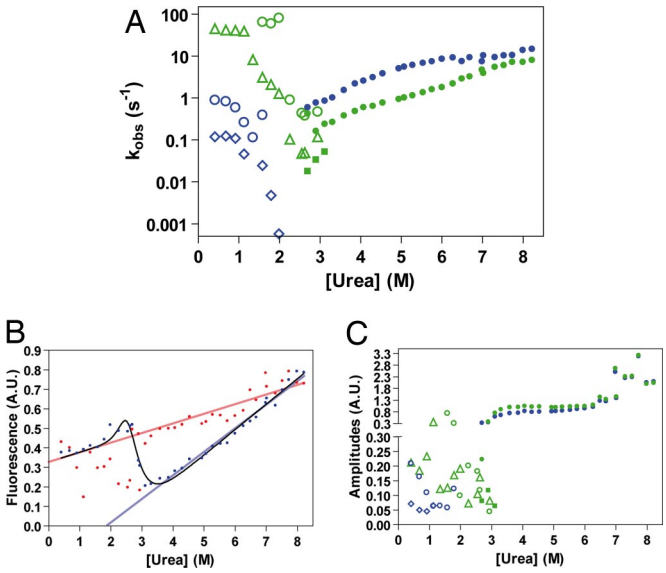

Fig. 2. Urea dependence of the kinetics monitored by stopped-flow fluorescence. (*A*) Urea dependence of the observed rate constants. Closed symbols indicate unfolding experiments; open symbols indicate refolding experiments. Phases associated with an increase in fluorescence for unfolding and a decrease for refolding are in blue. Phases associated with a decrease in fluorescence for unfolding and an increase for refolding are in green. (*B*) End-point analysis. Starting points (point at $t = 0$ s as estimated from the curve fit) are in red, end points (point at $t = \infty$ as estimated from the curve fit) are in blue. The urea dependence of the fluorescence of the native state and the unfolded state is shown by red and blue lines, respectively. The urea dependence of the end points resembles the fluorescence-monitored equilibrium denaturation curve (solid line). (*C*) Urea dependence of the amplitudes, colors as in *A*.

predicted in molecular dynamics simulations of ankyrin repeat folding (20) and has now been observed for the proteins myotrophin (14) and gankyrin (R. D. Hutton, A. R. Lowe, and L.S.I., unpublished results) in addition to D34. However, two other ankyrin repeat proteins p16 (21) and Notch (22) appear to fold via unique pathways, which presumably reflects the distribution of stability across the repeats. Thus, when the repeats within a protein have similar stabilities, multiple pathways may then arise if the energy barriers to their folding are also of a similar energy. By contrast, when some repeats have significantly greater stabilities than others, there is a unique folding pathway that is robust (i.e., it is not altered on perturbation such as mutation or changes in solution conditions like denaturant concentration). Finally, we discuss possible reasons for the different unfolding behavior of D34 under equilibrium and kinetic conditions and for the different kinetic unfolding mechanisms of the N- and C-terminal halves of the protein.

Results and Discussion

D34 Unfolds with Biphasic Kinetics. Unfolding of D34 was monitored by tryptophan fluorescence. The unfolding traces correlate with the equilibrium denaturation curve of D34 in that the fluorescence increases in a fast phase and then decreases in a slower phase, suggesting the formation and decay of a hyperfluorescent intermediate (supporting information (SI) Fig. S1). At urea concentrations outside the transition region the data can be fitted to the sum of two exponential phases (Fig. 2*A*). For both phases, the plot of the logarithm of the rate constant as a function of urea concentration shows downward curvature. Curvature can indicate a change in the position of the rate-limiting transition state along the reaction coordinate relative to the ground state of the transition. Downward curvature may be explained by a broad transition state barrier model assuming a smooth movement of the top of the transition state with increasing urea concentrations (23) in accordance with Hammond behavior. An alternative model views two sequential transition states separated by a high-energy intermediate (24). At increasing urea concentrations the rate-limiting barrier switches from one transition state to the other. Interestingly, at intermediate urea concentrations there is a slight upward curvature in the limb of the slower unfolding phase. Upward curvature cannot be explained by these models and is thought instead to indicate a switch between parallel pathways (25–28).

Refolding Kinetics Indicate That There Are Multiple Intermediates. On refolding, a hyperfluorescent intermediate is populated but the traces are more complex than the unfolding traces and more than two exponential phases are required to fit the data (Fig. S1*B*). In the transition region (refolding into 2.25–3 M urea) there is an increase in fluorescence that can be fitted to the sum of two exponential functions. At urea concentrations between 0.9 M and 2.25 M, in addition to increasing fluorescence, there is a decrease in fluorescence that can be fitted to either one exponential or to the sum of two exponentials. At urea concentrations <0.9 M, there is a monophasic increase in fluorescence followed by a biphasic decrease in fluorescence. The unfolding and the corresponding refolding phases should have opposite amplitudes, the magnitude of which is the same. However, it appears that the unfolding amplitudes are much bigger than refolding amplitudes (Fig. 2*C*), and analysis of the fluorescence start and end points indicates that a burst phase associated with a large increase in fluorescence occurs within the instrument dead time (Fig. 2*B*). D34 contains 22 proline residues, and the slowest observed refolding phase ($\approx$0.1 s^{-1}) could be limited by proline isomerization. It is of the same order of magnitude as proline isomerization phases observed for other proteins, including ankyrin repeats (29, 30), and the reaction is speeded up 2- to 3-fold in the presence of the peptidyl-prolyl isomerase cyclophilin A (data not shown).

Protein Concentration Dependence of Refolding. The effect of varying protein concentration on the refolding kinetics can be used to determine whether the reaction is limited by aggregation or oligomerization. Aggregation has been reported to give rise to downward curvature (or rollover) in the refolding limb (31). We found that changing the protein concentration affects the refolding of D34 when the reaction is performed in 0.41 M urea (Fig. S2). At protein concentrations <3 μM the rate constants do not change, but at protein concentrations between 4 μM and 6 μM the reaction is slowed down significantly. Interestingly, it appears that the burst phase in refolding, as identified by the missing signal in the end-point analysis, is also affected by the protein concentration because at higher protein concentrations the recorded transient starts at much lower relative fluorescence intensity than at lower protein concentrations. Monitoring refolding by absorbance at 600 nm gives a trace that is similar to that observed by fluorescence but somewhat slower. Thus, at protein concentrations of 4 μM and above, there appears to be some transient aggregation. The refolding reaction is not affected by protein concentration when it is performed at urea concentrations of 0.9 M and above (data not shown). The unfolding kinetics did not change over a 6-fold range of protein concentration (data not shown), and gel filtration data indicate that the protein is monomeric under these experimental conditions.

CD and Double-Jump Experiments Reveal Further Kinetic Phases. To investigate whether the observed transitions involve concomitant changes in secondary and tertiary structure, the kinetics was next monitored by using far-UV CD as a probe of α-helical structure. We found that unfolding traces fit well to the sum of two exponential functions and the rate constants agree with those obtained by fluorescence (Fig. S3). The two phases have significant and similar amplitudes, suggesting that, as in the

equilibrium studies, the hyperfluorescent species is associated with (or coupled to) a significant change in α-helical structure and therefore involves the unfolding of repeats.

The refolding traces monitored by CD fit well to the sum of three exponentials and the inclusion of a fourth exponential did not improve the fit. However, the rate constants obtained do not agree with those determined from fluorescence experiments. Efforts to fit the CD data by using rate constants fixed at the values obtained from fluorescence experiments failed, suggesting that there are additional phases not detected by fluorescence. All three phases monitored by CD have significant amplitudes, suggesting that they correspond to refolding of significant populations and/or parts of the protein structure. Furthermore, unlike the fluorescence data, no major burst phase could be observed from the end-point analysis of the CD data (Fig. S3*B*). In summary, the unfolding kinetics monitored by CD and fluorescence are in agreement and the amplitudes monitored by CD are consistent with unfolding occurring via an intermediate containing approximately half of the ankyrin repeats structured and the other half unstructured, similar to the equilibrium unfolding intermediate. The end-point analysis and the noncoincidence of the refolding rate constants observed by fluorescence and CD suggest that the refolding reaction has significantly greater complexity than the unfolding reaction.

Sequential mixing (double-jump) experiments were also performed to investigate further the kinetics of D34 (Fig. S4). Interrupted unfolding experiments (in which the protein is first unfolded and then, after a variable delay time, it is refolded) indicate that there is a "hidden" refolding phase of similar rate but of opposite sign to one of the phases observed by fluorescence and it is therefore masked in the single-jump refolding experiment. Interrupted refolding experiments (in which the protein is first refolded and then, after a variable delay time, it is unfolded) reveal that folding occurs rapidly to a native-like state and the conversion of this state to the native state occurs slowly and is spectroscopically silent. At very long refolding delay times, the unfolding kinetics of the protein is in good agreement with that observed in the single-jump unfolding experiment.

The Two Unfolding Phases Are Affected Differently by N-Terminal and C-Terminal Mutations. To map out the structural changes occurring in the kinetic phases described above, we examined the response of D34 to mutation at sites throughout its structure. Only the unfolding kinetics of the mutants is described because this reaction appears to be homogenous, whereas the refolding kinetics is highly complex and the phases cannot be assigned unambiguously (see Fig. S5). Previously we measured the equilibrium unfolding behavior of seven valine-to-alanine mutants, each located at position 18 of their respective ankyrin repeat (19) (Fig. 1). V420A, in repeat 1, had negligible effect on the stability of the protein and is therefore not analyzed further here. The remaining six mutations were significantly destabilizing: V486A, V519A, V585A, V651A, V717A, V750A, located in repeats 3, 4, 6, 8, 10, and 11, respectively. A number of other variants were constructed (Fig. 1), including mutations in repeats 2, 5, 7, 9, 11, and 12 (L456A, L540A, L606A, L687A, L753A, and V782G). L606A was prone to proteolysis, a problem we have observed for another mutant in this region of the protein (W600Y), and therefore could not be analyzed further. Also, mutants were constructed that were intended to stabilize the most C-terminal repeats, either by replacing residues with ankyrin consensus residues (a triple mutant G767Q/I780D/V785L) or by using the program FoldX (32) that predicts the change in stability on mutation (V750F, N761Y, T768P). However, the ankyrin repeats of D34 are already very consensus-like and none of the mutations was found to be significantly stabilizing and most were very destabilizing.

The two unfolding phases are affected by the mutations in a way that is reminiscent of the effects of the mutations on equilibrium unfolding (19). Thus, the behavior of the mutants can be grouped according to whether they are located in the N- or C-terminal half of the protein. N-terminal mutants affect only the fast phase, which corresponds to the unfolding of the native state to the intermediate, suggesting that the N-terminal moiety is at least partly unfolded in the transition state for the reaction (Fig. 3). Interestingly, the mutants L456A, V486A, and V519A, in the N-terminal half of the protein, not only change the rate of the reaction but also change the shape of the limb associated with this phase, resulting in less curvature. The slow unfolding phase, corresponding to the unfolding of the intermediate to the denatured state, is not affected by

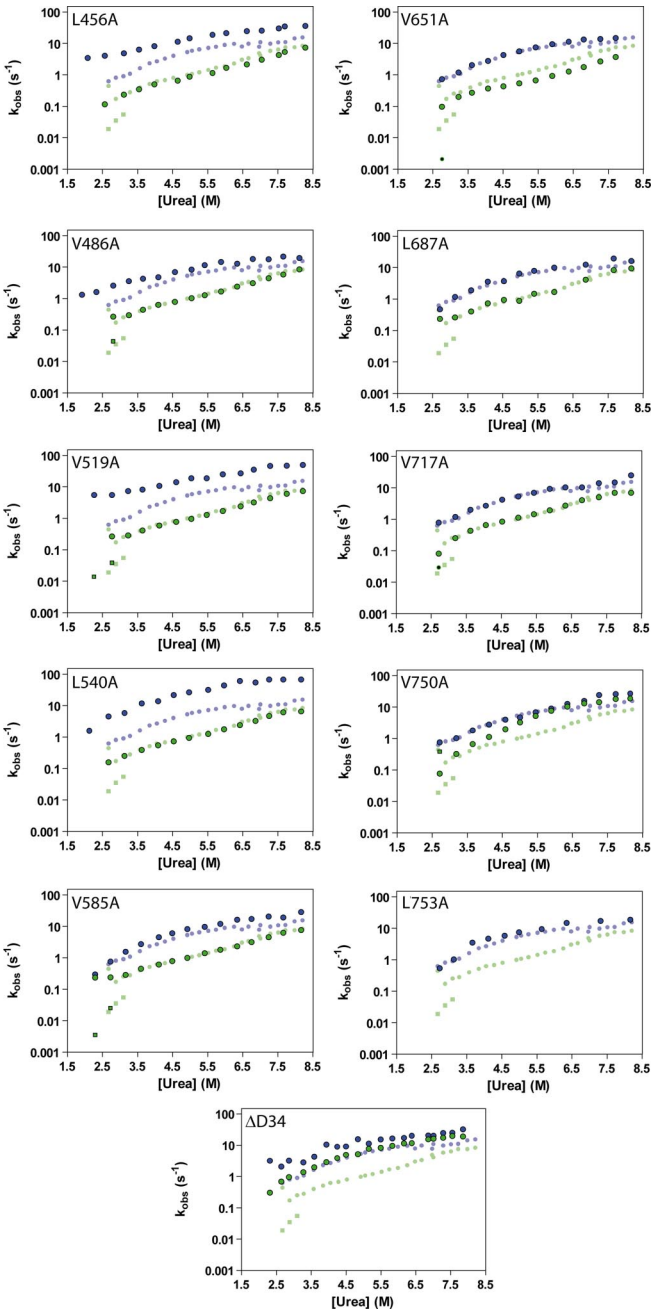

Fig. 3. The effect of mutations on the unfolding kinetics of D34. A set of representative mutants are shown. The rate constants for the mutant protein are in black and blue and black and green, and the rate constants for wild type are in pale blue and pale green (colors as in Fig. 2*A*).

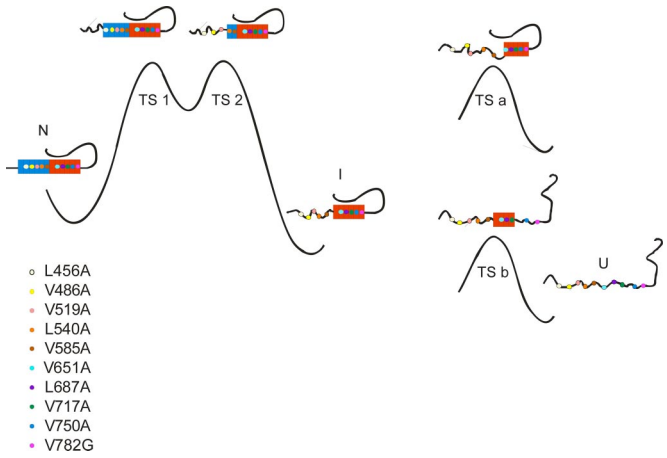

Fig. 4. Scheme for the kinetic unfolding mechanism of D34. Unfolding occurs via an intermediate (I) in which the N-terminal six (approximately) repeats are unfolded and the C-terminal six repeats are folded. The reaction between the native state (N) and I proceeds via sequential transition states (TS1 and TS2). The reaction between I and the unfolded state (U) proceeds via one of two pathways in which the transition state has either late (pathway a) or early (pathway b) C-terminal repeats folded. The positions of representative mutations shown in Fig. 3 are denoted by colored dots.

N-terminal mutations, which would be consistent with this moiety being already unfolded in the ground state of the reaction. C-terminal mutations affect the unfolding kinetics in a different way from N-terminal mutations (Fig. 3). These mutations do not affect the fast unfolding phase. V750A speeds up the slow unfolding phase and changes the shape of the limb, V651A slows down this phase and L687A and V717A overlap with the wild type. Their behavior is consistent with the slow phase corresponding to the unfolding of an intermediate with structured C-terminal repeats and unstructured N-terminal repeats.

The unfolding kinetics of the mutants obtained by monitoring ellipticity at 222 nm agrees with that obtained by fluorescence (data not shown). Interestingly, whereas at equilibrium the intermediate is destabilized by C-terminal mutations resulting in the population of different intermediates, the lack of change in the amplitudes of the unfolding phases of these mutants compared with the wild type suggests that the unfolding reaction proceeds through the same intermediate in wild-type and mutant proteins. This point is discussed further below. The equilibrium unfolding intermediate of wild-type D34 has a structured C-terminal half and an unstructured N-terminal half; the unfolding amplitudes monitored by CD and the effects of the mutations are consistent with a similarly structured kinetic unfolding intermediate.

Data for the Transition Between N and I Are Consistent with a Sequential Barriers Model. It is possible to discern a pattern in the kinetics of wild type and mutants of D34. We emphasize, however, that the limited number of mutations allows us to propose only low-resolution pictures for the transition state structures of the two unfolding phases. The downward curvature in the limb for the faster unfolding phase, and the changes in the curvature as a result of mutations in the N-terminal moiety (Fig. 3), can be interpreted in terms of a sequential barriers mechanism (24) for the unfolding of this part of the protein (Fig. 4). According to this mechanism, there are two distinct transition states with a high-energy intermediate in between. At lower urea concentrations, the less-structured transition state (TS2) is rate-limiting; the more-structured transition state (TS1) becomes more destabilized with increasing urea concentration than does TS2, and therefore TS1 becomes rate-limiting. The data are consistent with a model in which TS2 has repeats 2–6 folded (as well as repeats 7–12 folded) and TS has only repeats 5 and 6 folded (as well as repeats 7–12 folded). Thus, mutations in repeats 2–4 (e.g., L456A, V486A and V519A) destabilize TS1 but not TS2 and therefore the switch from TS2 to TS1 as the rate-determining energy barrier occurs at a lower urea concentration compared with the wild type, and the unfolding arm of such a mutation looks more linear than that of the wild type. By contrast, mutations in repeats 5–6 (L540A, V585A) destabilize both TS1 and TS2, and therefore the unfolding arm displays similar curvature to that of the wild type. Because the unfolding arms of these two mutants are parallel to that of the wild type, Φ-values can be calculated from the change in the rate constants, and the Φ-value will be the same for TS1 and TS2. The Φ-value is calculated from:

$$\phi = 1 - \frac{\Delta\Delta G_{\mathrm{TS-N}}}{\Delta\Delta G_{\mathrm{I-N}}} = 1 - \frac{RT \cdot ln\left(\frac{k'_u}{k_u}\right)}{\Delta\Delta G_{\mathrm{I-N}}}$$

where $\Delta\Delta G_{\mathrm{I\text{-}N}}$ is the change on mutation in the free energy of unfolding between the native state and the intermediate, $\Delta\Delta G_{\mathrm{TS\text{-}N}}$ is the change in the free energy of the transition state relative to the native state on mutation, and k_u and k'_u are the rate constants of unfolding for wild type and mutant, respectively. $\Delta\Delta G_{\mathrm{I\text{-}N}}$ was calculated as the product of the weighted mean equilibrium *m*-value (between N and I) of wild-type and all N-terminal mutants and the change in the midpoint of unfolding (between N and I) on mutation. Φ-values were compared at 3.5 M, 5.5 M, and 8.5 M urea by using the measured rate constants of unfolding at those concentrations and they were found to be similar to one another (±0.05), as expected because wild-type and mutant unfolding arms are parallel to each other. L540A results in a large $\Delta\Delta G_{\mathrm{I\text{-}N}}$ (5.7 kcal·mol^{-1}) and exhibits a relatively small but significant increase in the rate constants for unfolding; the Φ-value obtained is 0.83. $\Delta\Delta G_{\mathrm{I\text{-}N}}$ for V585A is smaller (2.8 kcal·mol^{-1}) and there is also a smaller change in the rate constants for unfolding on mutation; the Φ-value obtained is 0.89. These high Φ-values indicate that the structures of TS1 and TS2 are nativelike in repeats 5 and 6. If repeats 2–4 were also fully folded in TS1 then we would expect the rate constants of unfolding for L456A, V486A, and V519A to overlay the wild-type values at high urea concentrations when TS1 is rate-limiting. Because they approach the wild-type values, but do not quite reach them, the interactions must be formed only in part in TS1. We emphasize that downward curvature can be interpreted using other models—namely movement along a broad transition state barrier or native state fraying (23). The physical picture is the same in all three, however: unfolding by peeling away of structure from the N terminus to the middle of the protein.

Data for the Transition Between I and U Are Consistent with Alternative Pathways. The upward curvature in the limb for the slower unfolding phase points to a parallel pathways model for unfolding of the intermediate (Fig. 4). The changes in the curvature as a result of mutations in the C-terminal moiety are consistent with a model in which repeats 8–12 are structured in the transition state for pathway a, and repeats 7–10 are structured in the transition state for pathway b. TSa is more compact than TSb and, therefore, pathway a is more populated at low urea concentrations, but TSa becomes more destabilized with increasing urea concentrations than does TSb; therefore, the flux shifts to pathway b at high urea concentrations. Mutations in repeats 9–10 (L687A, V717A) destabilize both TSa and TSb, and consequently the unfolding arm of such a mutant has a shape and rates similar to the wild type (Fig. 3). Mutation of repeats 11 and 12 has a different effect: V750A and V782G (repeats 11 and 12) destabilize only TSa and consequently pathway a is never populated. Thus, the unfolding arm of such a mutant displays no upward curvature (see V750A in Fig. 3). Several other mutations in repeats 11 or 12—V750F, L753A, T768P,

G767Q/I780D/V785L—were found to be highly destabilizing (as judged by equilibrium measurement). For these mutants we see only one unfolding phase, of decreasing fluorescence, corresponding closely in rate to the faster (N-I) phase of the wild type (see L753A in Fig. 3). This result can be explained if the mutation is so destabilizing that the intermediate no longer accumulates in the unfolding reaction (the rate of decay of I is faster than its formation), and consequently, we can only observe the unfolding of N and not the subsequent unfolding of I. It appears that these mutants display a more extreme version of the V750A behavior: for V750A, the I-U arm is speeded up relative to that of wild type, it shows downward curvature in the urea dependence, and consequently it has almost the same profile as the N-I arm. For the more destabilizing L753A, if the I-U arm likewise has downward curvature but is faster still, then it will become kinetically silent. Finally, the variant ΔD34 provides a nice illustration of the model. In ΔD34 we deleted the long loop that proceeds the ankyrin repeats (Fig. 1). The loop folds back and packs onto the C-terminal repeats as well as the late N-terminal repeats, and equilibrium measurement indeed shows that the truncation destabilizes both C- and N-terminal moieties (19). The loop will only contribute to the stability of TSa and not TSb because the loop cannot fold back onto the repeats when the most C-terminal repeats are unfolded as they are in TSb. The kinetics of ΔD34 is consistent with this effect (Fig. 3): The N-I arm resembles that of the late N-terminal mutant L540A—the curvature is similar to that of wild type and the rates are faster than wild type; the shape of the I-U arm resembles those of the other C-terminal mutants V750A and V782G, but the rates are faster still. In contrast to L753A where the I-U transition is no longer detected because the rate of decay of I is faster than its formation, the I-U transition is observed for ΔD34 because both N-I and I-U transitions are speeded up and so the rate of decay of I is still slower than its formation.

Interestingly, for V651A (repeat 8) the unfolding of the intermediate is slower than that for wild type. One possible explanation is that TSb is more destabilized than the native state by the mutation, a scenario that would arise if there were nonnative interactions or over-packing in the transition state.

Complex Refolding Kinetics of D34. By contrast with the unfolding kinetics, the refolding kinetics of D34 is much harder to dissect. At least three refolding phases can be discerned in the traces obtained by fluorescence, the slowest of which behaves in interrupted unfolding experiments in a manner consistent with rate-limiting proline isomerization. The urea dependences of the three refolding rate constants do not result in clearly distinguishable refolding limbs. Moreover, with the exception of the fast phase the rate constants obtained by CD are not in agreement with those obtained by fluorescence. The apparent discrepancy could arise if there are phases of opposite signs but similar rate constants, as we identified in the interrupted unfolding experiments. The end-point analysis indicates that there is also a burst-phase intermediate in refolding. Thus, there may be multiple intermediates populated in the refolding reaction that are not populated in the unfolding reaction because they are destabilized at high urea concentrations. Finally, the interrupted refolding experiments show that the native state is acquired on a slower time scale than that observed in the direct refolding experiments. Such behavior will arise if the denatured state ensemble has nonnative peptidyl proline bond(s) and can fold rapidly to a nativelike intermediate from which slow isomerization to the native state occurs, as has been observed for other proteins (33, 34). Because there appears to be no measurable population of molecules that acquires the native state on a fast time scale, then either there are multiple proline residues that give rise to the effect or there is a *cis* peptidyl proline bond in the native state in solution (all are *trans* in the crystal form).

The protein concentration dependence of the refolding reaction suggests an oligomerization event that occurs under strongly native conditions (0.4 M urea) (31). Oligomerization could take place by domain swapping, according to which one protein molecule exchanges a structural domain with an identical partner. It is possible that, on refolding, the repeats of one molecule could zip up in an intermolecular fashion from a partly folded intermediate state by domain swapping with another molecule; computational studies have suggested such behavior (20). Moreover, the fact that at higher protein concentrations (>4 μM) there is a phase that starts at a much lower fluorescence intensity than that observed at lower protein concentrations (where we detect a burst phase by end-point analysis) would suggest that any domain swapping takes place at a very early stage in the reaction, either in the denatured state or in the burst phase intermediate.

Equilibrium versus Kinetic Unfolding Mechanisms: A Comparison. Because the unfolding kinetics is relatively simple, these data, rather than the refolding kinetics, are the main focus of our discussion. We observe an unfolding intermediate at equilibrium and in the kinetics, and the two have similar properties. They are both hyperfluorescent and the CD data obtained for the wild-type protein are consistent with the kinetic intermediate having approximately half of the repeats folded, as is the case for the equilibrium intermediate. Another similarity between the intermediates is the behavior of destabilizing mutations in the N-terminal moiety. These affect only the fast unfolding phase, corresponding to the transition from the native state to the intermediate, and this result indicates that the N terminus is at least partly unfolded in the kinetic intermediate, as for the equilibrium intermediate. We were interested to see the response of the unfolding kinetics to mutations in the C-terminal moiety. To a first approximation, only the slow unfolding phase is affected by these mutations, consistent with this transition corresponding to the unfolding of an intermediate containing a folded C-terminal moiety. A key question is whether the kinetic intermediate behaves in the same way as the equilibrium intermediate in response to C-terminal mutations, that is, does destabilization of the C terminus by mutation give rise to the cooperative unfolding of more repeats in the transition from the native state to the intermediate and thereby an intermediate with fewer folded repeats, as observed at equilibrium (19)? The relative amplitudes of the two unfolding phases monitored by CD do not change on mutation, suggesting that the kinetic intermediate retains approximately the same number of folded repeats on C-terminal mutation

One can rationalize the different behavior of D34 under equilibrium versus kinetic conditions and also the different kinetic mechanisms of the N-terminal moiety versus the C-terminal moiety, in the following way. Under equilibrium conditions, a C-terminal mutation destabilizes the wild-type intermediate and results in a different intermediate being predominant, one in which that site is unstructured. Thus, as the position of the mutation moves closer to the C terminus, the unfolding intermediate comprises a smaller number of folded C-terminal repeats. Under kinetic conditions, the unfolding reaction of wild-type D34 also proceeds from N to U via an intermediate (I) that resembles the equilibrium intermediate. Mutations in the C-terminal moiety destabilize I but do not result in the accumulation of different intermediates comprising fewer folded repeats. One possible explanation for this behavior is that the energy barriers that follow these later intermediates are low and because these intermediates lie after the rate-determining step, they are therefore kinetically silent. Given sufficient destabilization, for example, with the mutation L753A, I also becomes kinetically silent and we can see only the unfolding of N and not the subsequent unfolding of I. The presence of alternative routes between I and U might also lead to differences in kinetic versus equilibrium behavior, for exam-

ple, additional (albeit high energy) intermediates. It would be interesting to use simulations to probe those regions of the unfolding reaction, like unstable intermediates, that are inaccessible experimentally. Because the C-terminal moiety folds and unfolds in the context of an unfolded N-terminal moiety, it behaves like a single-domain ankyrin repeat protein, having a high degree of symmetry and consequently more than one unfolding pathway accessible to it. By contrast, there are no alternative pathways in the reaction between N and I because the N-terminal moiety folds and unfolds in the context of a folded C-terminal moiety, which therefore acts as a "seed" and confers a unique directionality on the process. The unzipping of the N-terminal moiety from repeat 1 to repeat 6 also makes sense of the sequential transition states that are observed in this unfolding reaction, having gradually fewer folded repeats.

Previous studies of ankyrin repeat proteins as well as the data presented in this work suggest that the energy landscape of repeat proteins is very rough with many intermediate and transition states (19, 35, 36). These states are very close in energy and therefore mild perturbations, such as mutations of single amino acids, can alter the distribution of these states significantly. In an earlier study we described this effect on intermediate species that populate during equilibrium unfolding. Here, we focused on the kinetics of unfolding, that is, on the transition states that represent the highest energetic barriers in the unfolding energy landscape, the peaks rather than the troughs. Interestingly, we come to the same conclusion as before: Small perturbations by single-point mutations change the energy differences of the observed states to such an extent that other transitions become rate-limiting or the flux distribution of competing pathways is changed.

Methods

Protein Expression and Purification. D34 was expressed and purified and the equilibrium stability was measured as described in ref. 19. All experiments were performed at 25°C in Tris·HCl buffer (pH 8), 150 mM NaCl, and 1 mM DTT or DTE.

Stopped-Flow. Fluorescence experiments were performed by using an Applied Photophysics SX-18MV stopped-flow instrument. The temperature of the observation cell was maintained with a waterbath. Excitation was at 280 nm by using a 2-nm excitation slit width. Emission was monitored >305 nm by using a glass cut-off filter. For unfolding experiments, protein in buffer was rapidly mixed (in a ratio of 1:10) with buffer containing various concentrations of urea between 2.5 M and 9 M. For refolding experiments, protein was denatured in buffer containing 4.5 M urea and incubated for at least 1 h at 25°C before mixing (1:10) with buffer containing various concentrations of urea between 0 M and 2.5 M. The final protein concentration was 2 μM. Approximately six traces were obtained at each denaturant concentration, and the averaged data were fitted to various exponential equations using Graphpad Prism 4.0.

Interrupted unfolding experiments were performed by mixing protein (36 μM) in buffer at a 1:5 ratio, followed by 1:5 mixing with buffer or with 1.5 M urea in buffer to initiate refolding at a final protein concentration of 1 μM in 0.75 M or 2 M urea, respectively. Interrupted refolding experiments were performed by incubating protein (36 μM) in 4.5 M urea for 1 h before mixing with 0.3 M or 1.5 M urea in buffer at a 1:5 ratio for refolding into final urea concentrations of 1 M and 2 M, respectively. After the delay time a second 1:5 mixing with 7 M or 6.8 M urea initiated unfolding at a final protein concentration of 1 μM in 6 M urea. Approximately three traces were obtained at each delay time and the averaged data for the different delay times were fitted globally by using Prism 4.0.

Kinetic circular dichroism experiments were performed on an Applied Photophysics pistar 180 stopped-flow instrument. Ellipticity was monitored at 222 nm. The experiments were performed at a protein concentration of 3 μM.

ACKNOWLEDGMENTS. We thank C. Dobson for use of CD, S. Perrett for helpful advice, and S. Schwitalla for help in purifying and analyzing proteins. The Itzhaki lab is supported by the Medical Research Council of the U.K. N.D.W. was supported by Carl Duisberg Stiftung (Germany).

1. Ferreiro DU, Walczak AM, Komives EA, Wolynes PG (2008) The energy landscapes of repeat-containing proteins: Topology, cooperativity, and the folding funnels of one-dimensional architectures. *PloS Comput Biol* 16;4(5):e 1000070.
2. Groves MR, Barford D (1999) Topological characteristics of helical repeat proteins. *Curr Opin Struct Biol* 9:383–389.
3. Kobe B, Kajava AV (2000) When protein folding is simplified to protein coiling: The continuum of solenoid protein structures. *Trends Biochem Sci* 25:509–515.
4. Andrade MA, Perez-Iratxeta C, Ponting CP (2001) Protein repeats: Structures, functions, and evolution. *J Struct Biol* 134:117–131.
5. Binz HK, *et al.* (2004) High-affinity binders selected from designed ankyrin repeat protein libraries. *Nat Biotechnol* 22:575–582.
6. Zahnd C, *et al.* (2007) A designed ankyrin repeat protein evolved to picomolar affinity to Her2. *J Mol Biol* 369:1015–2108.
7. Stumpp MT, Forrer P, Binz HK, Pluckthun A (2003) Designing repeat proteins: Modular leucine-rich repeat protein libraries based on the mammalian ribonuclease inhibitor family. *J Mol Biol* 332:471–487.
8. Main ER, Xiong Y, Cocco MJ, D'Andrea L, Regan L (2003) Design of stable alpha-helical arrays from an idealized TPR motif. *Structure* 11:497–508.
9. Binz HK, Stumpp MT, Forrer P, Amstutz P, Plückthun A (2003) Designing repeat proteins: Well-expressed, soluble and stable proteins from combinatorial libraries of consensus ankyrin repeat proteins. *J Mol Biol* 332:489–503.
10. Ferreiro DU, *et al.* (2007) Stabilizing IkappaBalpha by "consensus" design. *J Mol Biol* 365:1201–1216.
11. Tripp KW, Barrick D (2007) Enhancing the stability and folding rate of a repeat protein through the addition of consensus repeats. *J Mol Biol* 365:1187–1200.
12. Wetzel SK, Settanni G, Kening M, Binz HK, Pluckthun A (2008) Folding and unfolding mechanism of highly stable full-consensus Ankyrin repeat proteins. *J Mol Biol* 376:241–257.
13. Parmeggiani F, *et al.* (2008) Designed armadillo repeat proteins as general peptide-binding scaffolds: Consensus design and computational optimization of the hydrophobic core. *J Mol Biol* 376:1282–1304.
14. Lowe AR, Itzhaki LS (2007) Rational redesign of the folding pathway of a modular protein. *Proc Natl Acad Sci USA* 104:2679–2684.
15. Bennett V, Baines AJ (2001) Spectrin and ankyrin-based pathways: Metazoan inventions for integrating cells into tissues. *Physiol Rev* 81:1353–1392.
16. Corey DP, *et al.* (2004) TRPA1 is a candidate for the mechanosensitive transduction channel of vertebrate hair cells. *Nature* 432:723–730.
17. Howard J, Bechstedt S (2004) Hypothesis: A helix of ankyrin repeats of the NOMPC-TRP ion channel is the gating spring of mechanoreceptors. *Curr Biol* 14:R224–R226.
18. Sotomayor M, Corey DP, Schulten K (2005) In search of the hair-cell gating spring elastic properties of ankyrin and cadherin repeats. *Structure* 13:669–682.
19. Werbeck ND, Itzhaki LS (2007) From the Cover: Probing a moving target with a plastic unfolding intermediate of an ankyrin-repeat protein. *Proc Natl Acad Sci USA* 104:7863–7868.
20. Ferreiro DU, Cho SS, Komives EA, Wolynes PG (2005) The energy landscape of modular repeat proteins: Topology determines folding mechanism in the ankyrin family. *J Mol Biol* 354:679–692.
21. Tang KS, Fersht AR, Itzhaki LS (2003) Sequential unfolding of ankyrin repeats in tumor suppressor p16. *Structure* 11:67–73.
22. Bradley CM, Barrick D (2006) The notch ankyrin domain folds via a discrete, centralized pathway. *Structure* 14:1303–1312.
23. Otzen DE, Oliveberg M (2002) Conformational plasticity in folding of the split beta-alpha-beta protein S6: Evidence for burst-phase disruption of the native state. *J Mol Biol* 317:613–627.
24. Bachmann A, Kiefhaber T (2001) Apparent two-state tendamistat folding is a sequential process along a defined route. *J Mol Biol* 306:375–386.
25. Matthews JM, Fersht AR (1995) Exploring the energy surface of protein folding by structure-reactivity relationships and engineered proteins: Observation of Hammond behavior for the gross structure of the transition state and anti-Hammond behavior for structural elements for unfolding/folding of barnase. *Biochemistry* 34:6805–6814.
26. Dalby PA, Oliveberg M, Fersht AR (1998) Movement of the intermediate and rate determining transition state of barnase on the energy landscape with changing temperature. *Biochemistry* 37:4674–4679.
27. Otzen DE, Oliveberg M (2002) Conformational plasticity in folding of the split beta-alpha-beta protein S6: Evidence for burst-phase disruption of the native state. *J Mol Biol* 317:613–627.
28. Wright CF, Lindorff-Larsen K, Randles LG, Clarke J (2003) Parallel protein-unfolding pathways revealed and mapped. *Nat Struct Biol* 10:658–662.
29. Mello CC, Bradley CM, Tripp KW, Barrick D (2005) Experimental characterization of the folding kinetics of the notch ankyrin domain. *J Mol Biol* 352:266–281.
30. Lowe AR, Itzhaki LS (2007) Biophysical characterisation of the small ankyrin repeat protein myotrophin. *J Mol Biol* 365:1245–1255.
31. Silow M, Oliveberg M (1997) Transient aggregates in protein folding are easily mistaken for folding intermediates. *Proc Natl Acad Sci USA* 94:6084–6086.
32. Schymkowitz J, *et al.* (2005) The FoldX web server: An online force field. *Nucleic Acids Res* 33:W382–W388.
33. Schreiber G, Fersht AR (1993) The refolding of cis- and trans-peptidylprolyl isomers of barstar. *Biochemistry* 32:11195–11203.
34. Galani D, Fersht AR, Perrett S (2002) Folding of the yeast prion protein Ure2: Kinetic evidence for folding and unfolding intermediates. *J Mol Biol* 315:213–227.
35. Barrick D, Ferreiro DU, Komives EA (2008) Folding landscapes of ankyrin repeat proteins: experiments meet theory. *Curr Opin Struct Biol* 18:27–34.
36. Ferreiro DU, Komives EA (2007) The plastic landscape of repeat proteins. *Proc Natl Acad Sci USA* 104:7735–7736.
37. Michaely P, Tomchick DR, Machius M, Anderson RG (2002) Crystal structure of a 12 ANK repeat stack from human ankyrinR. *EMBO J* 21:6387–6396.